Relationship Between the Formation of Hollow Bead Defects and Hydrogen Assisted Cold Cracking

I. H. Brown, G. L. F. Powell, V. M. Linton
The University of Adelaide, Adelaide, South Australia

A. Kufner
F-H Konstanz, Konstanz, Germany

Abstract

The relationship between the occurrence of Hollow Bead Defects in root runs of pipeline welds, weld metal microsegregation, and hydrogen assisted cold cracking is investigated. Hollow Bead Defects and hydrogen assisted cold cracking are both found to occur in welds containing segregated regions of manganese and silicon. An experimentally substantiated model for the formation of Hollow Bead Defects is proposed.

Keywords: welding, hydrogen assisted cold cracking, hollow bead

Introduction

Oil and gas pipelines are commonly welded using the stove-pipe technique, a manual metal arc welding technique using cellulosic electrodes. Cellulosic electrodes provide good penetration and high travel speeds and hence high productivity.

Hollow Bead Defect occurs in the root pass of pipeline welds and is commonly described as an elongated linear porosity located in the root pass of a pipeline weld.

Cantin [1] and Barkow [2] both attempted to experimentally determine the conditions under which Hollow Bead occurs. Cantin [1] found that the most important factor for the occurrence of Hollow Bead Defects was a fast weld travel speed combined with high welding current. The major gas in the Hollow Bead pore is hydrogen, which has been rejected from the super-saturated liquid ahead of the solid-liquid interface. On the basis of these findings Cantin postulated that the hydrogen gas rejected by the saturated liquid ahead of the solid-liquid interface accumulates in one single gas bubble, which is enclosed by columnar grains growing parallel to the welding direction. However no evidence was provided to substantiate this mechanism.

Hydrogen assisted cold cracking (HACC), also referred to as delayed cracking or cold cracking, occurs in the weld metal of high strength welds. The factors leading to HACC are well known [3], namely the simultaneous presence of a critical concentration of diffusible hydrogen, a residual or applied stress and a susceptible microstructure. In addition, the cracking normally occurs at a temperature below 200°C.

Since the major gas inside the Hollow Bead Defect is hydrogen, it seems likely that there could be a relationship between the occurrence of Hollow Bead Defects and HACC.

In pipeline welding, Hollow Bead Defects are not seen as a major defect if their length and size is within the limits specified in the relevant Australian Standard [4]. This is a consequence of the rounded nature of the pore. However these limits may need reassessment if it could be shown that the conditions for the formation of Hollow Bead Defects are similar to those for the appearance of hydrogen assisted cold cracking (HACC).

Experimental

Welded samples of two line-pipe steels, API 5L X70 (X70) and API 5L X80 (X80) were examined. The samples manufactured from 8.3mm thick API 5L X70 steel plate were supplied by Cantin. Further test plates were manufactured from 9mm thick API 5L X80 steel plate under conditions likely to produce Hollow Bead. The composition of both steels is given in Table 1.

Table 1: Chemical compositions of X70 [1] and X80 [5] plates

	C	Mn	Si	Ni	Cr	Mo	Al	Nb	Ti
X70	0.09	1.56	.33	.022	.017	.002	.03	.04	.012
X80	0.09	1.7	.38	-	-	.035	.05	.08	0.25

All welds were single pass root runs with no filling runs and were produced using cellulosic electrodes (AWS E6010/AS E4110). These electrodes are commonly used for the field welding of line pipe. Welds were produced in an automated manual metal arc welding machine designed to simulate the stovepipe welding technique using a travel speed of 500mm/min, a welding voltage of approximately 30V and a welding current of 190A giving a heat input of 0.66kJ/mm.

Joints in the 200mm x 450mm steel plates were prepared to the Australian Standard AS2885.2 – 2002 with a root face of 1.6 – 2.1mm, a root gap of 1.3 – 1.6mm and a bevel angle of 30°. The welding was done at room temperature with no preheat.

After welding, the plates were x-rayed to locate Hollow Bead Defects. Cross sections of those welds containing Hollow Bead Defects were prepared using standard metallographic techniques for examination using optical light microscopy. The samples were examined after etching with 2% Nital, and then repolished and etched in LePera's reagent [5] Nital was used to reveal the phases resulting from the solid-state transformation, whereas LePera's reagent was used to reveal the microsegregation resulting from liquid to solid transformation.

The samples were further analyzed using a FEI/Phillips XL30 FESEM field emission scanning electron microscope on etched and unetched samples, and a Cameca SX51 electron microprobe was used on unetched samples for x-ray analysis and x-ray mapping.

Results

Segregation at the Weld Centreline
Visibly sound welds produced using the welding parameters described above were x-rayed, and Hollow Bead Defects were found in all x-rayed welds.

A transverse section of a Hollow Bead Defect is shown in Figure 2. Although not discernable at this magnification a crack emanates from the defect towards the top surface of the weld.
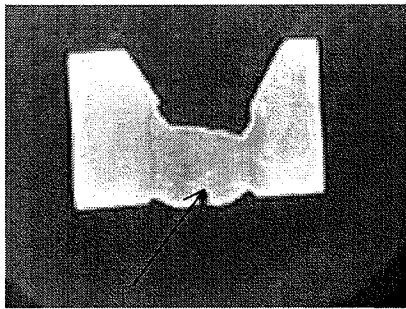

Figure 2. Transverse section of Hollow Bead Defect in X70 steel with crack initiation point arrowed. Magnification x1

When etched with LePera's reagent, all of the transverse sections showed long columnar grains growing from the parent material towards the centre of the weld. However, in the region of the Hollow Bead pore, the microstructure changed. There was a triangular region above the pore that appeared to contain equiaxed grains. The apex of the triangle was on the centreline of the weld and the region was symmetrical either side of the pore. This feature was observed in the X70 and X80 samples. Figure 3 is an optical micrograph where this feature has been highlighted.
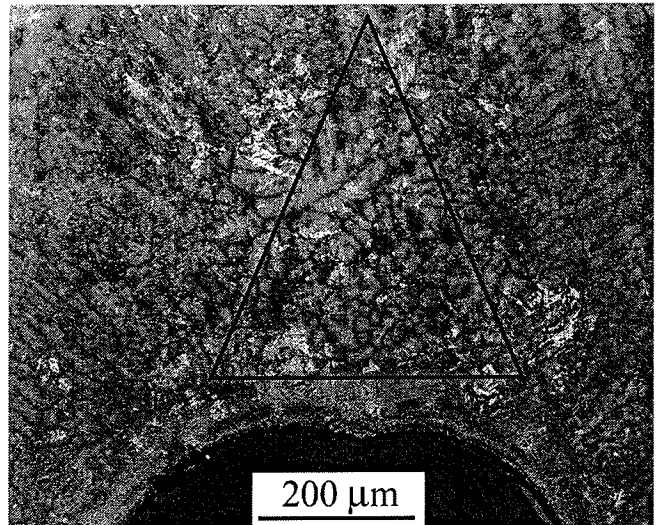

Figure 3: The microstructure at the weld centerline above a Hollow Bead Pore in X70 steel: Segregation is indicated by the darker etched regions of the cellular dendrite boundaries The triangular region referred to in the text is marked. The cellular dendrites are approximately 20μm in diameter. Etchant LePera's reagent.

A crack is evident along the centreline of the weld shown in Figure 4. The crack follows a zigzag pattern along the boundaries of the cellular dendrites as indicated by the black arrows. The growth direction of the cellular dendrites at the mid height of the weld is horizontal; in the upper region is inclined slightly upwards towards the centre of the weld and in the lower part of the weld is inclined downwards towards the Hollow Bead pore. This indicates the change of the direction of the heat extraction and hence the direction of solidification.

To identify the segregated elements in the weld centreline, x-ray line scans were carried out across the crack along the white line shown in Figure 4 using an x-ray analytical facility attached to an SEM. The scans were made with a voltage of 20kV, a dwell time of 100 seconds per point and 128 points per line. A typical line scan is shown in Figure 5.
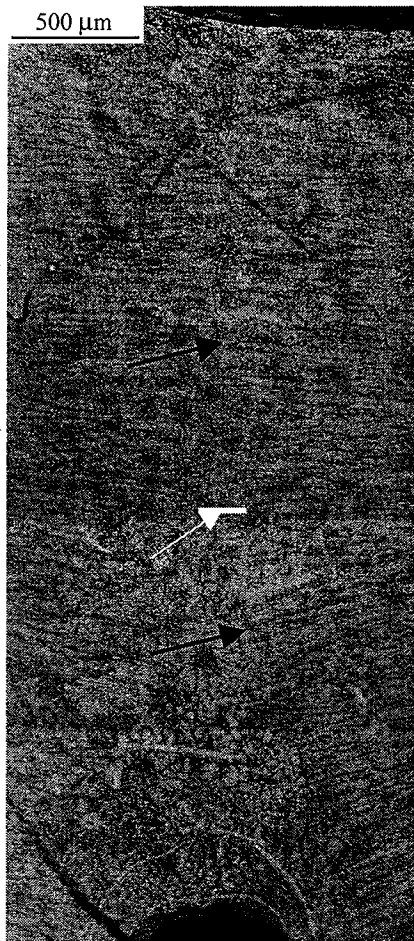
500 µm

Figure 4: Collage of optical micrographs extending from a hollow bead pore to the weld surface showing cracking along the segregation at the centerline of the weld. The position of the x-ray line scan (Figure 5) is shown by the white arrowed line. Etchant: LePera's reagent.

Figure 5: Linescan across weld centerline showing increased concentrations of manganese and silicon.

Manganese and silicon are clearly segregated at the weld centreline, with manganese in particular showing a high intensity peak. All samples which contained Hollow Bead Defects showed similar characteristics:

Investigation of segregation surrounding a crack

Figure: 6 SEM collage of a crack emanating from a Hollow Bead Defect (bottom) and following a path through oxide inclusions (arrowed). Etchant: LePera's reagent.

Figure 6 is a collage of micrographs taken using the back-scattered electron mode of the SEM. The sample has been etched in LePera's reagent. The figure shows that the crack has grown in a band where the material was smoother after etching in LePera's reagent than the surrounding areas. The crack is tight, follows a staircase pattern and is branched. It can also be seen that the crack travels along a path running between inclusions.

To identify the elements segregated around the crack, x-ray maps of the crack shown in Figure 6 were collected using electron probe microanalysis.
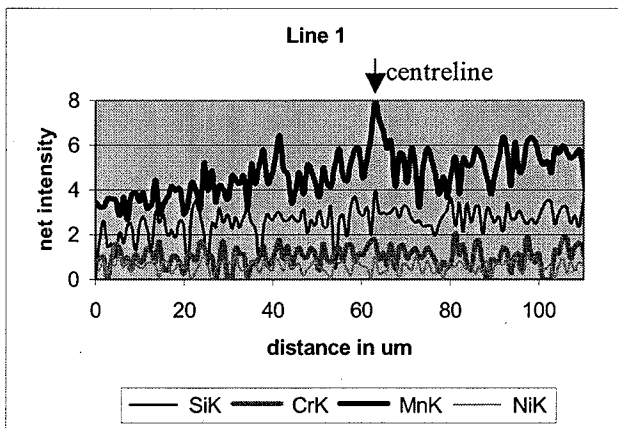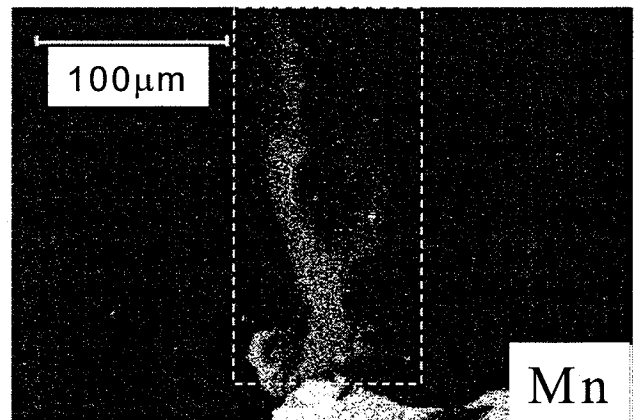
Figure 7: X-ray map of the cracked region using the microprobe. The manganese segregation appears in the outlined area as the lighter region. (Unetched)
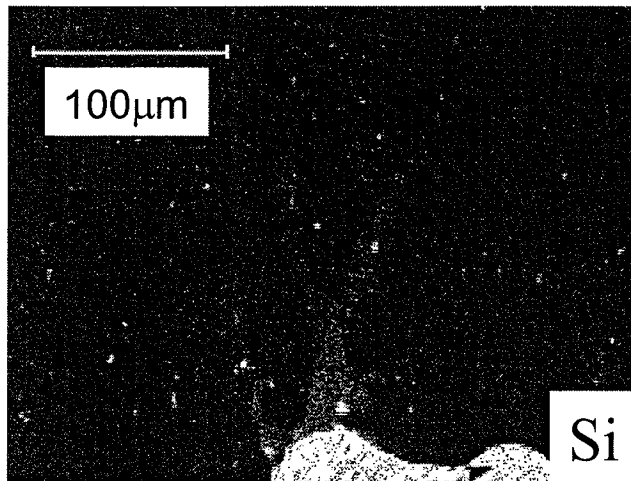

Figure 8: X-ray map of the cracked region using the microprobe. The silicon segregation appears as the lighter region. (Unetched)

The maps (Figures 7 and 8) show that the crack follows a segregated region which contains considerably higher manganese and considerably higher silicon contents than the bulk of the weld metal. The segregated region corresponds to the smooth region in Figure 6.

The nominal concentrations of silicon, manganese and iron were confirmed using x-ray line scans across the segregated area containing the crack shown in Figure 6. These confirmed the results shown in the area scans Figures 7 and 8. The scans were collected at approximately the mid length of the crack. In the segregated region the silicon content increased from approximately 0.2% to 0.5%. and the manganese content increased from approximately 1% to 5% with a subsequent decrease in the iron content from approximately 99% to 95%.

Investigation of Hollow Bead Pore
Cantin [1] suggested that the growth direction around the Hollow Bead Defects is parallel to the welding direction (which is also the orientation of the Hollow Bead Pore). This theory was supported by Powell et al. [6], whose research on elongated gas pores in welds, observed cellular dendrites growing parallel to the gas pores. To substantiate Cantin's hypothesis, it was considered important to further investigate the structure surrounding the Hollow Bead pores.
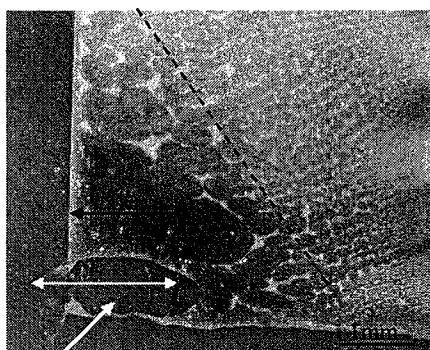
Hollow Bead Pore   Black arrow indicates cellular

To investigate the solidification mode around the Hollow Bead Defects, longitudinal sections of welds containing Hollow Bead pores were cut along the centreline of the pores. The samples were polished and etched with LePera's reagent to reveal the microstructure as shown in Figure 9.

Figure 9: Microstructure of a longitudinal section of a hollow bead pore. The pore is at the bottom left of the image and the black arrow indicates the direction of welding. The lighter etched regions indicate intercellular segregation. Etchant: LePera's reagent

The section shows that in the region to the left of the dotted line in Figure 9 the cellular dendrites grow parallel to the welding direction, which is the growth direction of the pore. Further away i.e. to the right of the dotted line in Figure 9, the columnar grains grow in a direction almost normal to the page i.e. almost at 90 degrees to the growth direction of the pore.

To substantiate these findings the inside surface of Hollow Bead pores were closely examined. Cross-section samples of welds containing Hollow Bead Defects were metallographically ground to the mid height of the pore, and the inside surface of the pores examined in the SEM.

On the internal surface of the pore, protrusions which were aligned in the longitudinal direction of the pore and the welding direction, were observed. These protrusions were also evident on the bottom surface of the pore. The protrusions do not run absolutely parallel to the elongated direction of the pore, but run slightly towards the centre of the pore. The distance between the protrusions is approximately 20μm, which corresponds to the diameter of the cellular dendrites as shown in Figure 3.

Discussion

Segregation surrounding a crack
A hydrogen assisted cold crack was found in the root pass of a weld in X70 steel. The crack was initiated at a Hollow Bead Defect. X-ray line and area scans revealed that the crack occurred in a region where the manganese and silicon contents were higher than in the surrounding weld metal. The localised increase in manganese and silicon content was a result of segregation at the cellular dendrite boundaries during the solidification of the weld metal [7]. This increase in the alloy content of these two elements increased the hardenability of these regions which increased their susceptibility to HACC

Scanning electron micrographs showed the crack path ran between oxide inclusions. This is expected because these inclusions would also be segregated to the cellular dendrite boundaries during solidification. It has previously been reported [8] that HACC follows these inclusions and that these oxide inclusions not only act as stress raisers but also as hydrogen traps, i.e. the residence time of diffusible hydrogen is longer at the inclusion than in other parts of the

microstructure. This leads to an increase in triaxial stresses around the inclusion which further increases the susceptibility to cracking.

Segregation associated with Hollow Bead Defect

With the chosen welding parameters, the production of Hollow Bead Defects in the welds was very reproducible. Every weld contained several Hollow Bead Defects, generally in the bottom part of the weld

The occurrence of Hollow Bead Defects corresponded with with the weld growth pattern shown in Figure 3.

The solidification mode of the welds is as described by Savage [9]. A transverse section of the solidification morphology is shown schematically in Figure 10. The cellular dendrites grow from the parent metal towards the centre of the weld, where they meet. The growth direction at the mid-height position of the weld is horizontal, whereas in the top section of the weld it is slightly upwards, and in the bottom section of the weld it is slightly downwards. In the welds with Hollow Bead Defects, a triangular shaped area just above or below the Hollow Bead, and generally towards the middle of the weld, was observed. In this area, the grains appeared to be equiaxed, but it could be shown by taking a longitudinal section through the Hollow Bead and etching in LePera's reagent, that they were in fact cellular dendrites growing in the direction of the Hollow Bead pore
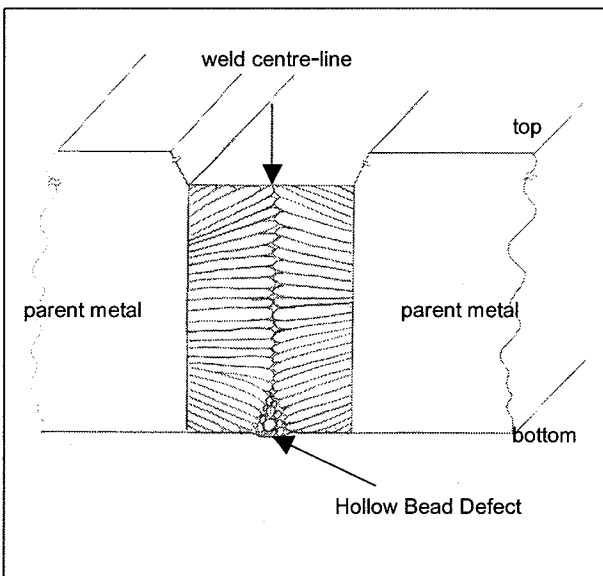

Figure 10: Schematic of a transverse cross section of a weld containing Hollow Bead Defect in the root pass.

Examination of the inside of the Hollow Bead pores, revealed protrusions on the inside surface. The distance between the protrusions was approximately 20µm, which is approximately the diameter of the cellular dendrites. These protrusions were almost parallel to the welding direction. It was shown by Powell [7] that these protrusions are regions of segregation at the cellular dendrite boundaries as a consequence of the lower liquidus temperature of the

enriched liquid. The protrusions point towards the centre of the pore. A model for the formation of Hollow Bead based on these findings, and supported by the hypothesis suggested by Cantin [1] is presented in Figure 11.

Cantin [1] showed that the gas inside Hollow Bead Defects is almost 100% hydrogen. The solutibility of hydrogen in the liquid phase of steel is higher than in the solid phase. Hydrogen was rejected from the supersaturated liquid phase ahead of the solid-liquid interface as the temperature decreased. The hydrogen accumulated in the form of hydrogen bubbles. These bubbles were forced towards the outer surface of the weld by the advancing solidification front, where they would normally escape. However, due to the high weld travel speeds and the high cooling rates involved in the present experiments, a layer of solid metal rapidly forms at the surface of the weld and the hydrogen cannot escape. The bubbles become encapsulated in a thin layer of the last metal to solidify, metal that is enriched in alloying elements and at the centreline of the weld bead.
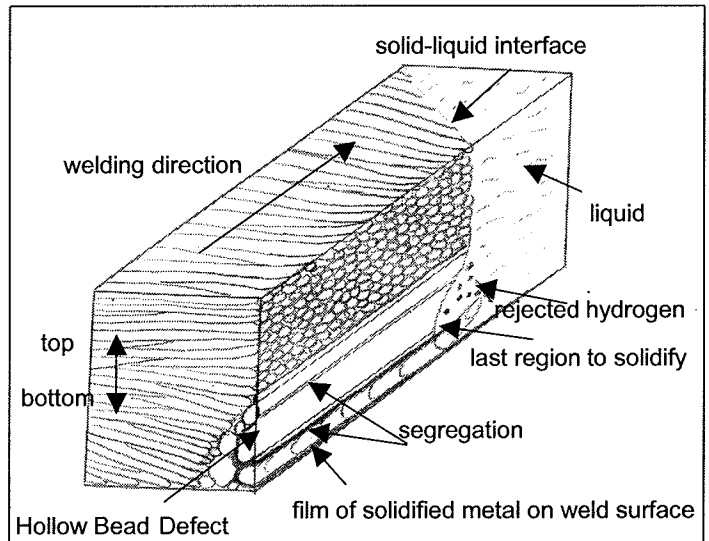

Figure 11: Transverse section of a schematic model for the formation of Hollow Bead Defects.

The Hollow Bead pore propagates in the direction of the solidification front, i.e. the welding direction as more and more diffusible hydrogen is rejected from the liquid metal.

The cellular dendrites next to the Hollow Bead pore are observed to be relatively large compared to the epitaxial grains growing from the parent metal. These grains were probably nucleated at the skin around the gas pore ahead of the epitaxial growth solidification front. They are located in the last metal to solidify at which stage the heat transfer is relatively slow, giving the grains sufficient time to develop their size.

In welding tests, conducted with the low travel speed, cellular dendrites growing parallel to the welding direction were not found. This suggests that growth in the direction of welding requires a high travel speed with a corresponding

high cooling rate. None of the specimens taken from the low weld travel speed welds (300mm/minute) showed either cellular dendrites parallel to the welding direction or Hollow Bead Defects. The cellular dendrites grew from the parent material towards the weld centreline. This was the case from the top of the weld to the bottom of the weld in all of samples (Figure 12).

Conclusion

From the results of the present research it has been possible to postulate a model for the formation of the Hollow Bead Defect. Previous research on Hollow Bead Defects has concentrated on the conditions for its formation rather than the mechanism of formation [1][2]. In agreement with that previous work, this work found that Hollow Bead Defects formed at higher weld travel speeds and higher welding currents. These welding conditions produce a change in the growth direction of the cellular dendrites from perpendicular to the welding direction towards the welding direction and also produce a line of segregation from the bottom to the top of the weld. In addition it was found that in the samples containing the Hollow Bead Defect the cellular dendrites surrounding the Hollow Bead Defect and the Hollow Bead Defect itself grew parallel to the welding direction. When welded at slower travel speeds and lower currents no change in growth direction or Hollow Bead Defect were detected.

A crack initiated at the surface of a Hollow Bead Defect and travelling to the weld surface was investigated. The crack followed the segregated regions at the centreline of the weld. The segregated regions were higher in manganese and silicon indicating that these regions would have higher hardenability. Therefore all of the factors necessary for the formation of a cold crack were present, hydrogen, residual stress due to solidification and regions of increased hardenability. The morphology of the crack reflected cold cracks previously investigated and reported [7] in that it was tight, branched and linked inclusions

References

1. G. M. D. Cantin, *An Investigation of the Formation of Hollow Bead Defects in Pipeline Field Welds*, PhD Thesis, 1998
2. A. G. Barkow, *New Welding Problem for Pipeliners*, The Oil and Gas Journal, 71 40-47 (1973)
3. P .H .M. Hart,., *Resistance to Hydrogen Cracking in Steel Weld Metals*. Welding Journal, 14-22 (1986)
4. AS2885.2, Pipelines - *Gas and liquid petroleum. Part 2*, Welding. Standards Australia, 2002
5. F. S. LePera, J. Met., 32, 38-39 (1980)
6. G. L. F. Powell, and P. G. Lloyd, *Characterisation of an Elongated Gas Pore in a Weld in Terms of Solidification Mechanics*. Prakt. Metallogr., 1995. **32**: p. 25-31
7. I. H. Brown, G. L. F. Powell, J. L. Davidson, V. M. Linton, *Cold Cracking and Segregation in Multi-pass Welds of a Quenched and Tempered Steel*, 6th Int. Conf. on Trends in Welding Research, Georgia USA, 2002.
8. Bhadeshia H., *Microstructure modelling in weld metal,* Mathematical modelling of weld phenomena 3, H. Cejrak ed., 650, 1997, 229 - 282.
9. Savage, W.F., *1980 Houdremont Lecture*. Welding in the world, 18(5/6), 89-114, 1980